

Caspase-8 dependent osteosarcoma cell apoptosis induced by proteasome inhibitor MG132

Xiao-Bo Yan^a, Di-Sheng Yang^a, Xiang Gao^a, Jie Feng^b, Zhong-Li Shi^b, Zhaoming Ye^{a,*}

^a Department of Orthopaedics, 2nd Affiliated Hospital, School of Medicine, Zhejiang University, 88 Jie Fang Road, Hangzhou 310009, Zhejiang, P.R. China

^b Institute for Orthopaedic Research, ZheJiang University, Hangzhou, P.R. China

Received 13 July 2006; revised 12 January 2007; accepted 21 March 2007

Abstract

Many researchers have reported that proteasome inhibitors could induce apoptosis in a variety of cancer cells, such as breast cancer cell, lung cancer cell, and lymphoma cell. However, the effect of proteasome inhibitors on osteosarcoma cells and the mechanisms are seldom studied. In this study, we found proteasome inhibitor MG132 was an effective inducer of apoptosis in human osteosarcoma MG-63 cells. On normal human diploid fibroblast cells, MG132 did not show any apoptosis-inducing effects. Apoptotic changes such as DNA fragment and apoptotic body were observed in MG132-treated cells and MG132 mostly caused MG-63 cell arrest at G₂–M-phase by cell cycle analysis. Increased activation of caspase-8, accumulation of p27^{Kip1}, and an increased ratio of Bax:Bcl-2 were detected by RT–PCR and Western blot analysis. Activation of caspase-3 and caspase-9 were not observed. This suggests that the apoptosis induced by MG132 in MG63 cells is caspase-8 dependent, p27 and bcl-2 family related.

© 2007 International Federation for Cell Biology. Published by Elsevier Ltd. All rights reserved.

Keywords: Proteasome inhibitor; Osteosarcoma; Apoptosis; p27^{Kip1}; Bcl-2; Caspase-8

1. Introduction

Osteosarcoma (OS) is the most common malignant bone tumor, mainly occurring in children and adolescents. Five-year disease-free survival has increased up to 60% with current protocols, including a combination of limb salvage and neoadjuvant chemotherapy (Bacci et al., 2000; Meyers et al., 1998). Despite the dramatic improvement, resistance to chemotherapy and metastatic spread are the two most important mechanisms responsible for the failure of current therapy (Bacci et al., 2000; Marina et al., 2004; Meyers et al., 1998; Scotlandi et al., 1996). Various studies suggest that an intrinsic resistance to apoptosis is one important mechanism by which OS cells escape therapeutic control (Chano et al., 2004; Fellenberg et al., 2003; Flintoff et al., 2004; Serra et al.,

2004). Therefore, new therapeutical strategies that bypass this resistance are necessary.

Recently, various researchers found that there was a 26S protease complex existing in eukaryote cells. This can degrade many kinds of proteins associated with immune recognition, transcript regulation, cell cycle progression, cell differentiation, stress response and apoptosis (Ferrari et al., 2005; Naujokat et al., 2000). The ubiquitin–proteasome system plays a key role in cell proliferation and cell death (Chen et al., 2000; Rock et al., 1994). It can be considered the fundamental system in the appropriate elimination of intracellular damaged proteins and in the rapid proteolysis of a variety of short-lived functional proteins (Ciechanover, 1998; Shah et al., 2001). We now know that the ubiquitin–proteasome pathway can increase amounts of cell cycle related proteins (p27^{Kip1}, p21^{Cip1}, p16, INK family, etc.) and tumor inhibition protein p53. It also can induce synthesis of death receptor and activation of caspase family. Inhibition of the ubiquitin–proteasome pathway by proteasome inhibitors has been an active area of

* Corresponding author. Tel./fax: +86 571 8702 2776.

E-mail address: zrgk5@zju.edu.cn (Z. Ye).

investigation. Proteasome inhibitors have been regarded as potentially cytotoxic agents against a variety of cancer cells *in vitro* and *in vivo*, including breast cancer cell, lung cancer cell and lymphoma cell (Cohen, 1997; Cohen et al., 1992; Ellis et al., 1991; Miller, 1997). Therapy of osteosarcoma using proteasome inhibitors is seldom reported.

The results described in this report showed that MG132 (z-Leu-Leu-Leu-CHO), an inhibitor of chymotrypsin-like activity of the proteasome, was an effective inducer of apoptosis in human OS MG-63 cells. Its effect was mediated by G₂–M-phase arrest, accumulation of p27^{Kip1} protein, and degradation of apoptosis-related proteins. Proteasome inhibitor is also a potent chemotherapeutic agent in the treatment of osteosarcoma.

2. Materials and methods

2.1. Reagents

z-Leu-Leu-Leu-CHO (MG132) was purchased from Sigma–Aldrich Chemical Co. (St. Louis, MO, USA) and dissolved in DMSO (10 mmol/L) as a stock solution. Mouse monoclonal antibodies specific for p27^{Kip1} (sc-1641) and caspase-3 were obtained from Sigma–Aldrich. MTT, mouse monoclonal antibodies specific for Bcl-2, rabbit polyclonal antibodies specific for Bax, caspase-8, caspase-9 and horseradish peroxidase-conjugated goat anti-mouse, horseradish peroxidase-conjugated goat antirabbit secondary antibody were obtained from Santa Cruz Biotechnology Inc. (Santa Cruz, CA, USA). Hoechst 33258 fluorescence kit was purchased from Beyotime Institute of Biotechnology (NanJing, China).

2.2. Cells and cell culture

The human OS cell line MG-63 and human diploid fibroblast cell line WI-38 used in this study were obtained from American Type Culture Collection (Manassas, VA, USA). Cells were grown in MEM medium (Gibco Life Sciences) supplemented with 10% (v/v) heat activated fetal bovine serum (Gibco Life Sciences) in a humidified atmosphere of 5% CO₂ and 95% air at 37 °C.

2.3. Cytotoxicity assay

MG-63 and fibroblastic cells were exposed to varying concentrations of MG132 for the indicated times, and then the cytotoxicity was determined by MTT assay, as described previously (Frankfurt and Krishan, 2003). Following incubation with drugs, 50 µl of 2 mg/ml MTT was added to each well, plates were incubated at 37 °C for 4 h and the medium was replaced with 150 µl of

DMSO. The absorbance in control and drug-treated wells was measured at 490 nm using a Dynatech MR7000 microplate reader. Each experimental data point represented the average value obtained from four replicates, and each experiment was performed in triplicate. The concentrations inhibiting growth by 50% (IC₅₀) were calculated using the linear regression analysis, with SPSS 11.5 software.

2.4. Fluorescence microscopy

To determine nuclear condensation by Hoechst 33258 staining, harvested MG-63 cells were washed in ice-cold PBS twice, fixed with 1 ml of 90% (v/v) cold ethanol for 10 min and then incubated with 3 µg/ml Hoechst 33258 for 5 min in the dark. Cells were then rinsed with distilled water, mounted on glass microscopic slides in 50% glycerol, and examined under a fluorescent microscope (Axioskop, Zeiss).

2.5. Electron microscopy

Cells were fixed with 2.5% glutaraldehyde, postfixed in 1% osmium tetroxide, and embedded in epoxy resin. Thin sections were stained in uranyl acetate and lead citrate, examined under a Philips TECNAI10 transmission electron microscope.

2.6. Determination of DNA fragmentation

For qualitative analysis of DNA fragmentation, cells were harvested after 24 h incubation with different concentrations of MG132 by centrifugation and lysed in lysis buffer consisting of 10 mM Tris–HCl (pH 7.4), 10 mM EDTA, and 0.1% of Triton X-100. They were incubated with RNase A and proteinase K at 37 °C for 60 min. After centrifugation, the soluble DNA fragments were precipitated by the addition of 0.5 volume of 7.5 M ammonium acetate and 2.5 volumes of ethanol. DNA pellets were dissolved in TE and loaded onto a 2.0% agarose gel and separated at 100 V for 45 min. DNA fragments were visualized after staining with ethidium bromide by transillumination under UV light.

2.7. Quantification of apoptosis

Cells were treated with various concentrations of MG132 for 24 h or 1.0 µmol/L MG132 for the indicated times before cells were harvested and fixed, and the DNA was stained by PI (propidium iodide) as described previously (Shah et al., 2001). Samples were then analyzed by flow cytometry (FACScan, BD Biosciences) and cells with sub-G1 DNA content were scored as apoptotic cells.

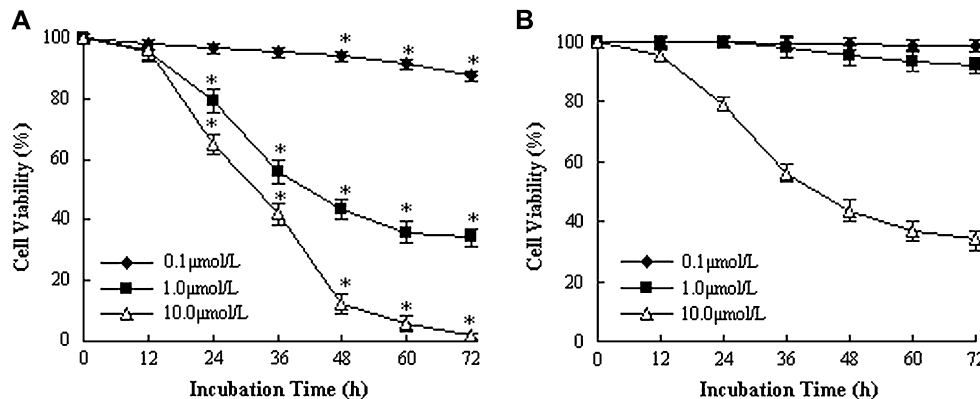


Fig. 1. Effect of MG132 on cell viability of MG-63 cells (A) and WI-38 cells (B). Cell viability was determined by MTT assay, as described in Section 2. Each point represents the $\bar{x} \pm s$ of three independent experiments (* $P < 0.05$, compared to the same point of WI-38 cells).

2.8. Cell cycle analysis

Cell cycle distribution was determined by DNA content analysis after PI staining. After exposure, MG-63 cells (10^6 per condition) were harvested and fixed with cold 70% ethanol at -20°C overnight. Cells were incubated with PI (50 $\mu\text{g}/\text{ml}$ in PBS containing 100 $\mu\text{g}/\text{ml}$ RNase A) at room temperature for 3 h. Flow cytometric determination of DNA content was analyzed by a FACScan (BD Biosciences) flow cytometer. For each sample, 20,000 events were stored. The fractions of the cells in G_0 – G_1 , S, and G_2 –M phases were analyzed using CELLQuest cell cycle analysis software.

2.9. RT–PCR analysis

RNA was prepared from cultured cells using the Trizol (Life Technologies) 1 ml. For RT–PCR analysis, total RNA was reverse transcribed with Mo-MLV

reverse transcriptase (Life Technologies) at 42°C for 1 h, followed by 10-min denaturation at 70°C and then quick cooling. The resulting cDNA was subjected to the PCR-based amplification with the following oligonucleotides: for human $p27^{\text{Kip1}}$, 5-ATGTCAAACGTGCGAGTGTC-3 and 5-CTCTGCAGTGCTTCTCCAAG-3; for human GAPDH, 5-ACCTGACCTGCCGTCTAGAA-3 and 5-TCCACCACCCTGTTGCTGTA-3. PCR was performed under the conditions: 5 min 94°C preincubation, followed by 30 cycles of denaturation (30 s, 94°C), annealing (1 min, 63°C), and extension (1 min, 72°C), followed by a final extension of 10 min at 72°C . PCR products were electrophoresed in a 2% neutral agarose gels and visualized by ethidium bromide staining.

2.10. Western blot analysis

Cells were harvested by trypsinization and then suspended in 30 μl of Western blot lysis buffer containing 50 mmol/L Tris–HCl (pH 7.5),

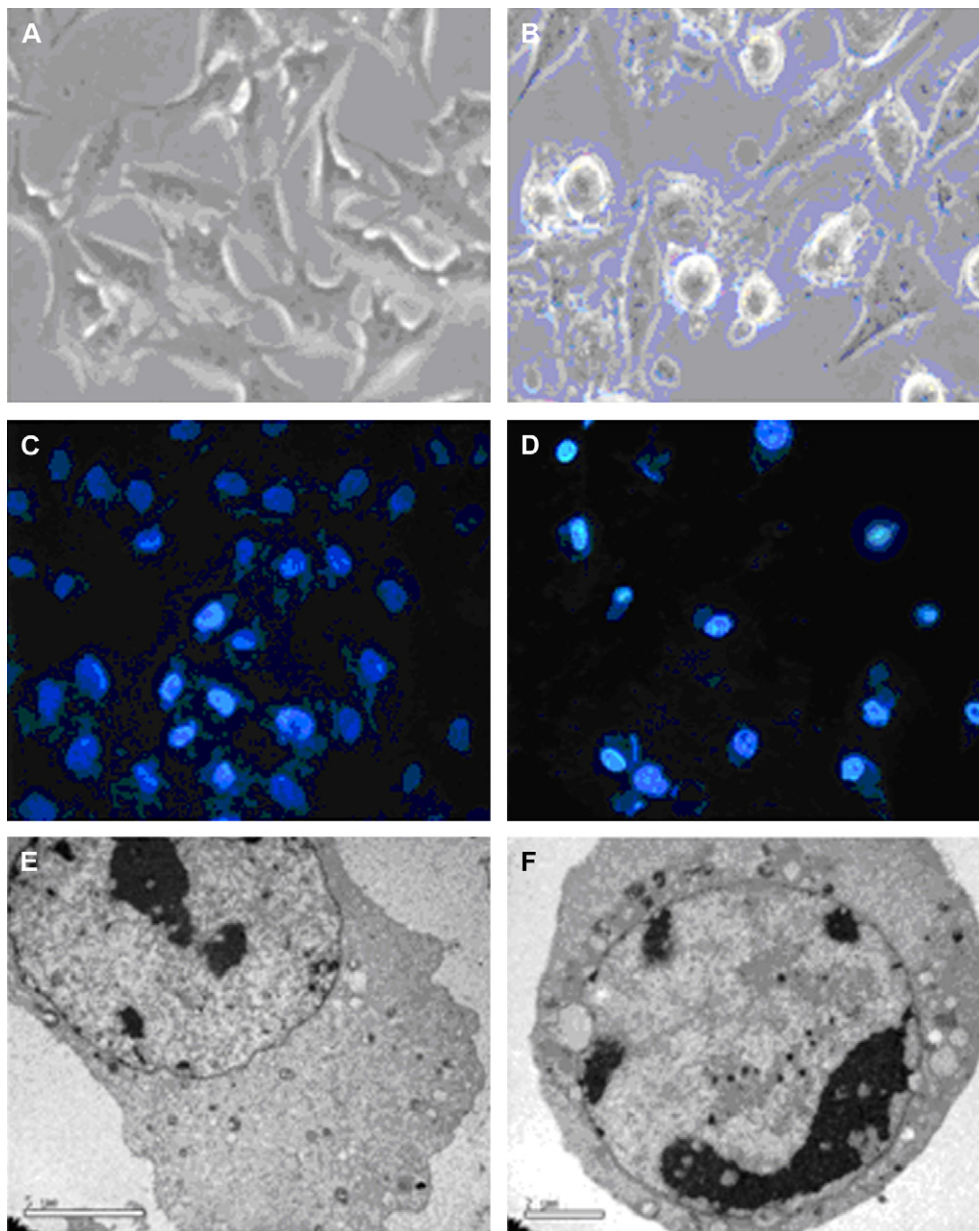


Fig. 2. Morphological change of MG-63 cells treated with proteasome inhibitor. MG-63 cells were observed by phase-contrast microscopy (A and B), by fluorescence microscopy after Hoechst 33258 staining (C and D) and by electron microscopy (E and F). MG-63 cells were incubated with 1.0 $\mu\text{mol}/\text{L}$ MG132, for the following time: no treatment (A, C and E) and 24 h of treatment (B, D and F).

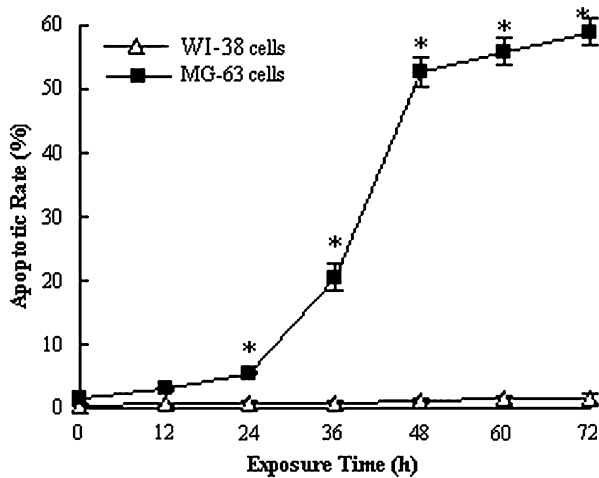


Fig. 3. Apoptotic rate of MG63 and WI-38 cells. MG-63 cells (■) and WI-38 cells (□) were incubated with 1.0 $\mu\text{mol/L}$ MG132 for 12–72 h, and cell apoptotic rate was quantitatively determined by flow cytometry. Each point represents the $\bar{x} \pm s$ of three independent experiments (* $P < 0.05$, compared to the same time of WI-38 cells).

150 mmol/L NaCl, 0.1% SDS, 1% NP-40, 0.5% sodium deoxycholate, 1 mmol/L PMSF, 100 $\mu\text{mol/L}$ leupeptin and 2 $\mu\text{g/ml}$ aprotinin at 0–4 $^{\circ}\text{C}$ for 15 min. After centrifugation at 1500 $\times g$ for 10 min at 0 $^{\circ}\text{C}$, the supernatants were collected, and the proteins were separated on 12% SDS-PAGE. After electrophoresis, protein blots were transferred to a nitrocellulose membrane. The membrane was blocked with 5% nonfat milk in TBST and incubated overnight with antibody at 4 $^{\circ}\text{C}$. After washing three times with TBST, the membrane was incubated at room temperature for 1 h with horseradish peroxidase-conjugated secondary antibody diluted with TBST (1:10,000). The detected protein signals were visualized by an enhanced chemiluminescence reaction system (Amersham, Arlington Heights, IL). Densitometric quantification of Bax/Bcl-2 rate was measured by Gel-Pro Analyzer 3.1 software.

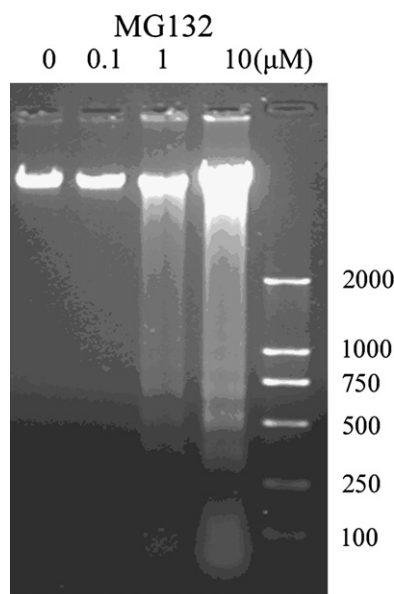


Fig. 4. DNA ladder of MG63 cells. Genomic DNA was extracted from MG-63 cells incubated with different concentrations of MG132 for 24 h, and subjected to 2% agarose gel electrophoresis.

2.11. Statistical analysis

Statistical significance was determined using Student's *t*-test and IC_{50} value was calculated using linear regression analysis, with SPSS 11.5 software. $P < 0.05$ was considered significant.

3. Results

3.1. Cell viability of MG-63 cells and WI-38 cells treated by MG132

The proteasome inhibitor, MG132, used in the present study efficiently blocked activity of proteasomes in eukaryotic cells (Rock et al., 1994). As shown in Fig. 1, MG132 markedly reduced the viability of MG-63 cells in a concentration-dependent manner (Fig. 1A). But WI-38 cells displayed a very weak sensitivity towards MG132 (Fig. 1B). The IC_{50} values of MG132 for MG-63 and WI-38 cells were $0.92 \pm 0.06 \mu\text{mol/L}$ and $9.13 \pm 0.12 \mu\text{mol/L}$, respectively.

3.2. Cell morphology of MG-63 cells treated with MG132

MG-63 cells treated with MG132 showed typical apoptotic changes. At 24 h after the proteasome inhibitor treatment, MG-63 cells gradually showed apoptotic morphological features (Fig. 2B, D): cell shrinkage, and nuclear condensation. Chromatin condensation, crescent nucleus and cytoplasmic vacuoles were also observed by transmission electron microscope (Fig. 2F).

3.3. Apoptotic rate of MG-63 cells and WI-38 cells induced by MG132

The apoptotic rate of MG63 cells increased significantly after cells were incubated with 1.0 $\mu\text{mol/L}$ MG132 for 24 h. The apoptotic rate was above 50% after 48 h. However, in WI-38 cells apoptotic rate did not increase compared to control, always below 5% (Fig. 3).

3.4. DNA ladder of MG63 cells treated with MG132

DNA isolated from MG63 cells cultured with 10 μM MG132 for 24 h showed the characteristic “ladder” pattern of apoptosis (Fig. 4). A comparison with molecular weight markers indicated that the fragments were multiples of approximately.

3.5. Cell cycle of MG-63 cells treated with MG132

MG132 treatment resulted in an increase of cell numbers at $\text{G}_2\text{--M}$ phase and a decrease of the cell numbers at G_1 phase in a concentration- and time-dependent manner (Fig. 5). 0.1 $\mu\text{mol/L}$ to 10 $\mu\text{mol/L}$ MG132 resulted in 27.7–72.1% of cells that arrested at $\text{G}_2\text{--M}$ phase (Fig. 5A), only 17.2% of cells at $\text{G}_2\text{--M}$ phase in the untreated cells (not shown). MG132 caused MG-63 cells to arrest at $\text{G}_2\text{--M}$ phase after

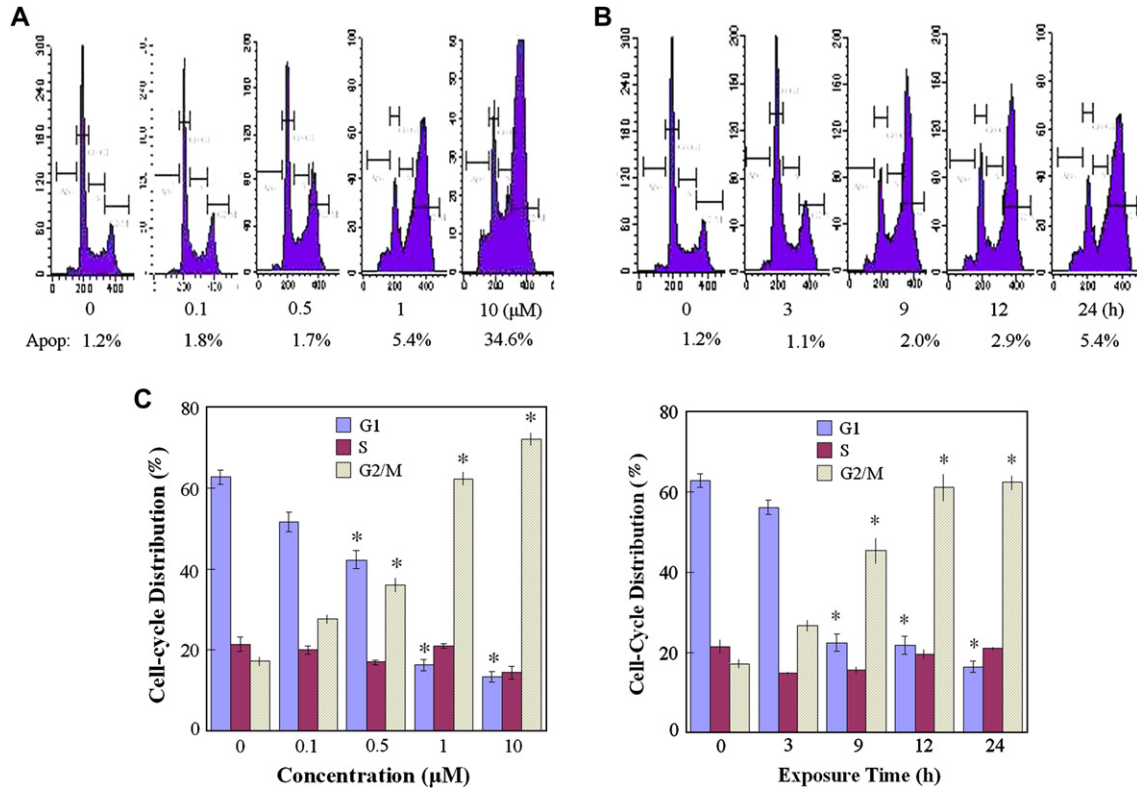


Fig. 5. MG132 induces G₂–M-phase arrest in MG-63 cells. MG-63 cells were exposed to various concentrations of MG132 for 24 h (A) or to 1.0 μmol/L MG132 for the selected time intervals (B). After exposure, cells (1 × 10⁶) were stained with propidium iodide as described in Section 2. The profiles of DNA content in each sample (measured by a flow cytometer) are presented in the top panel. Each bar standing for cell cycle distributions is presented in the bottom panel representing the $\bar{x} \pm s$ of three independent experiments (**P* < 0.05, compared to control).

9 h exposure, and the cell numbers at G₂–M phase gradually increased over longer exposure time (Fig. 5B).

3.6. Expression of p27^{Kip1} protein in MG63 cells treated with MG132

MG132 increased the transcriptional and translational level of p27^{Kip1} in a time-dependent manner in MG-63 cells. We found the mRNA of p27^{Kip1} increased 8 h after MG132 treatment (Fig. 6A), as did the protein level (Fig. 6B).

3.7. Apoptosis related protein expression in MG63 cells treated with MG132

After exposure to MG132, expression of caspase-3, -8, -9, Bax and Bcl-2 in MG-63 cells were tested. Caspase-8 was cleaved 48 h after MG132 treatment. The amount of cleaved caspase-8 increased with the increase of the concentration of MG132, but caspase-3 and -9 were not cleaved all the time (Fig. 7A, B). Cleaved caspase-3 and -9 was not observed. It was also found that Bcl-2 decreased and Bax increased as time passed. We measured the optical density of these bands and found that the Bax: cl-2 ratio increased in a time-dependent manner (Fig. 7C, D).

4. Discussion

Presently, the ubiquitin–proteasome system is paid close attention. Ubiquitin-mediated protein degradation is an important

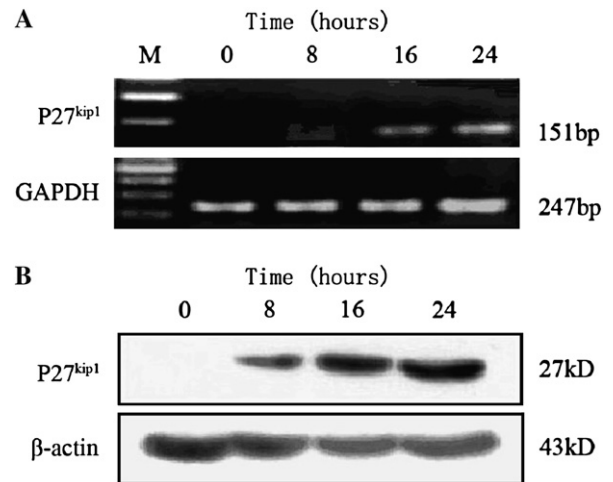


Fig. 6. Transcription of p27 mRNA and expression of p27 protein in MG-63 cells treated with proteasome inhibitor MG132. MG63 cells were treated with 1.0 μmol/L MG132 for 0, 8, 16, and 24 h. Total RNA was isolated from cells and RT–PCR was performed. Cell proteins were collected and Western blot was performed as described in Section 2.

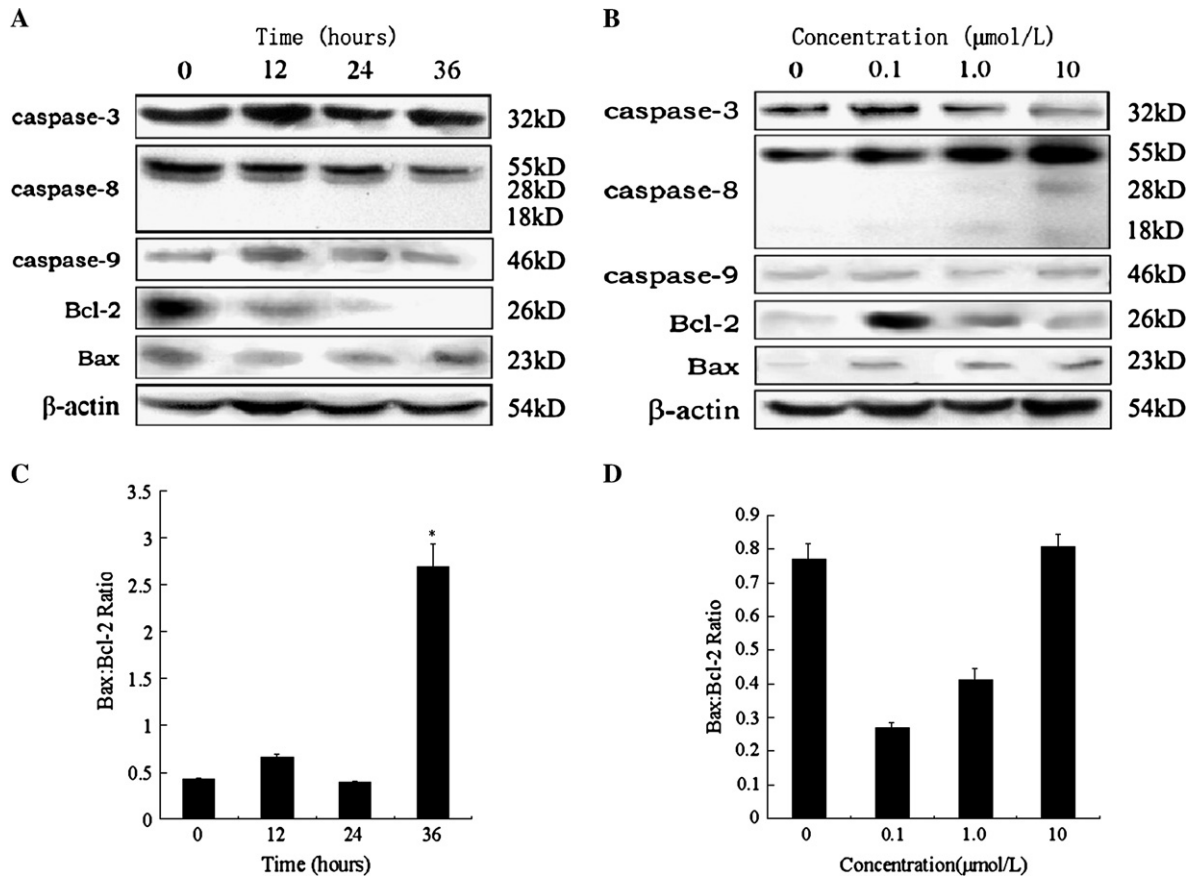


Fig. 7. Expression of caspase-3, -8, -9, Bax and Bcl-2 in MG-63 cells treated with MG132. MG-63 cells were exposed to 1.0 $\mu\text{mol/L}$ MG132 for indicated time or different concentrations of MG132 for 48 h. Cell lysates were separated by 12% SDS–PAGE electrophoresis. Protein bands were detected by Western blot analysis. β -actin was used as an equal loading control. Densitometric quantification of Bax:Bcl-2 ratio in MG132-treated MG63 cells was measured by Gel-Pro Analyzer 3.1 software (* $P < 0.05$, compared to control group).

part of numerous cellular processes, including cell-cycle regulation, signal transduction, gene transcription and apoptosis (Hershko, 1997; Liu et al., 2003). The ubiquitin–proteasome system is also an important regulator of cell growth and apoptosis. The potential of specific proteasome inhibitors to act as novel anti-cancer agents is currently under intensive investigation. Several proteasome inhibitors exert anti-tumor activity *in vivo* and potently induce apoptosis in tumor cells *in vitro*, including those resistant to conventional chemotherapeutic agents.

Apoptosis or programmed cell death is an intrinsic cell death program that is involved in the regulation of various physiological and pathological processes. Several reports have shown a close correlation between apoptosis and the inhibition of the ubiquitin–proteasome pathway (Emanuele et al., 2002; Frankel et al., 2000; Kelley et al., 2004). The findings presented in this research demonstrated that MG132, a member of the class of proteasome inhibitors, inhibited proliferation of OS cells. The percentage of cells at G_2 –M phase increased by up-regulating the concentration of MG132. 10 $\mu\text{mol/L}$ MG132 resulted in 72.1% cells accumulating at G_2 –M phase, with an apoptotic rate of 34.6%; but with 1.0 $\mu\text{mol/L}$ MG132 only about 60% of cells accumulated at G_2 –M phase after 24 h incubation and the apoptotic rate was only 5.4%.

Some studies demonstrated that G_2 –M phase accumulation was associated with downregulation of $p27^{\text{Kip1}}$ (Devlin et al., 2003). Nahreini et al. (2003) reported that partial proteasome inhibition triggered apoptosis in neuroblastoma cells with G_2 –M phase arrest and decreased level of $p27^{\text{Kip1}}$. Fujii et al. (1999) showed that 100 μM cisplatin induced MDA-231 human breast tumor cells to accumulate in G_2 –M phase while downregulating $p27$. However, $p27^{\text{Kip1}}$ is a member of the universal cyclin-dependent kinase inhibitor (CDKI) family, which is degraded by the proteasome. Proteasome inhibitor will decrease the degradation of $p27^{\text{Kip1}}$ and increase its expression. Moreover, apoptosis induced by proteasome inhibitor generally is accompanied by the accumulation of $p27^{\text{Kip1}}$ (An et al., 1998). In our study, MG132 increased the transcriptional and translational level of $p27^{\text{Kip1}}$ in MG-63 cells, which is consistent with recent reports that overexpression of $p27^{\text{Kip1}}$ protein leads to apoptosis in various cancer cell lines (Wang et al., 1997). Accumulation of $p27^{\text{Kip1}}$ protein might play an important role in apoptosis.

Generally, we know that there are two pathways in apoptosis: the cell surface death receptor pathway and the mitochondria-initiated pathway. In the cell surface receptor pathway, activation of caspase-8 following its recruitment to the death-inducing signaling complex is the critical event that

transmits the death signal. In the mitochondrial-initiated pathway, caspase-9 is activated first. Then it activates downstream caspases such as caspase-3, -6 and -7. Finally, activation of caspases during apoptosis results in the cleavage of critical cellular substrates, including poly(ADP-ribose) polymerase (PARP) and lamins (Budihardjo et al., 1999; Coffey et al., 2001; Wang and Lenardo, 2000).

Shinoura et al. (2001) reported that expression of P27^{Kip1} enhanced Fas ligand- or caspase-8-mediated apoptosis. Zhou et al. (2006) demonstrated proteasome inhibitors could decrease Fas-like inhibitor protein (FLIP) protein levels in tumors, resulting in increased apoptosis signaling due to increased caspase-8 activation. In this study, we found that caspase-8 was activated in MG-63 cells treated with MG132 for 48 h (Fig. 6). When 40 $\mu\text{mol/L}$ z-VAD-fmk, a broad spectrum caspase inhibitor, was added, caspase-8 was not activated (data not shown). This suggests that the induction of apoptosis in MG-63 cells by MG132 is caspase-8 dependent. Downregulation of Bcl-2 and upregulation of Bax was also observed in a time-dependent manner. But activation of caspase-9 and -3 was not observed even after cells were treated with 10 $\mu\text{mol/L}$ MG132 for 48 h (Fig. 6).

Hougardy et al. (2006) demonstrated that MG132 plus rhTRAIL enhanced caspase-8 and caspase-3 activation, with concomitant cleavage of X-linked inhibitor of apoptosis (XIAP) in HeLa cells. Lauricella et al. (2003) treated Saos-2 cells with MG132 and found that MG132 induced fragmentation of procaspase-3 and production of the active form of caspase-3 but was unable to induce fragmentation of procaspase-8. However, we found the opposite results on MG-63 cells. Saos-2 cells lack p53 and contain a nonfunctional form of pRb. MG-63 cells lack p53 gene but have functional pRb. p53 and the retinoblastoma protein (pRb) are products of tumor-suppressor genes, which are fundamental in the control of cell proliferation. The expression level of pRb phosphorylation is important to MG-63 cells (Merli et al., 1999). De Blasio et al. (2003) hypothesized a cross-talk between pRb and PARP. It is known that non-caspase proteases are able to interact with apoptosis via the caspase pathways (Johnson, 2000). We thought induction of the mitochondrial pathway not to be involved in apoptotic effects of MG132, and that activated procaspase-8 may directly activate PARP by the expression of RB gene. When the activation of procaspase-8 was inhibited, the accumulation of p27 and pRb protein dephosphorylation could not induce apoptosis alone.

In conclusion, we found that proteasome inhibitor MG132 was able to induce apoptosis in osteosarcoma MG-63 cells. The apoptosis was accompanied by activation of caspase-8, accumulation of p27 at the transcriptional and translational level, and increased ratio of Bax:Bcl-2. Activation of caspase-3 and caspase-9 was not observed.

References

An B, Goldfarb RH, Siman R, Dou QP. Novel dipeptidyl proteasome inhibitors overcome Bcl-2 protective function and selectively accumulate the cyclin-

- dependent kinase inhibitor p27 and induce apoptosis in transformed, but not normal, human fibroblasts. *Cell Death Differ* 1998;5:1062–75.
- Bacci G, Ferrari S, Bertoni F, Ruggieri P, Picci P, Longhi A, et al. Long-term outcome for patients with nonmetastatic osteosarcoma of the extremity treated at the istituto ortopedico rizzoli according to the istituto ortopedico rizzoli/osteosarcoma-2 protocol: An updated report. *J Clin Oncol* 2000; 18(24):4016–27.
- Budihardjo I, Oliver H, Lutter M, Luo X, Wang X. Biochemical pathways of caspase activation during apoptosis. *Annu Rev Cell Dev Biol* 1999;15: 269–90.
- Chano T, Mori K, Scotlandi K, Benini S, Lapucci C, Manara MC, et al. Differentially expressed genes in multidrug resistant variants of U-2OS human osteosarcoma cells. *Oncol Rep* 2004;11(6):1257–63.
- Chen F, Chang D, Goh M, Klibanov SA, Ljungman M. Role of p53 in cell cycle regulation and apoptosis following exposure to proteasome inhibitors. *Cell Growth Differ* 2000;11(5):239–46.
- Ciechanover A. The ubiquitin–proteasome pathway: on protein death and cell life. *EMBO J* 1998;17(24):7151–60.
- Coffey RN, Watson RW, Fitzpatrick JM. Signaling for the caspases: their role in prostate cell apoptosis. *J Urol* 2001;165:5–14.
- Cohen GM. Caspases: the executioners of apoptosis. *Biochem J* 1997;326: 1–16.
- Cohen JJ, Duke RC, Fadok VA, Sellins KS. Apoptosis and programmed cell death in immunity. *Annu Rev Immunol* 1992;10:267–93.
- De Blasio A, Musmeci MT, Giuliano M, Lauricella M, Emanuele S, D'Anneo A, et al. The effect of 3-aminobenzamide, inhibitor of poly (ADP-ribose) polymerase, on human osteosarcoma cells. *Int J Oncol* 2003;23(6):1521–8.
- Devlin AM, Solban N, Tremblay S, Gutkowska J, Schurch W, Orlov SN, et al. HCaRG is a novel regulator of renal epithelial cell growth and differentiation causing G2M arrest. *Am J Physiol Renal Physiol* 2003;284(4):F753–62.
- Ellis RE, Yuan JY, Horvitz HR. Mechanisms and functions of cell death. *Annu Rev Cell Biol* 1991;7:663–98.
- Emanuele S, Calvaruso G, Lauricella M, Giuliano M, Bellavia G, D'Anneo A, et al. Apoptosis induced in hepatoblastoma HepG2 cells by the proteasome inhibitor MG132 is associated with hydrogen peroxide production, expression of Bcl-Xs and activation of caspase-3. *Int J Oncol* 2002;21(4): 857–65.
- Fellenberg J, Dechant MJ, Ewerbeck V, Mau H. Identification of drug-regulated genes in osteosarcoma cells. *Int J Cancer* 2003;105(6):636–43.
- Ferrari S, Smeland S, Mercuri M. Neoadjuvant chemotherapy with high-dose ifosfamide, high-dose methotrexate, cisplatin, and doxorubicin for patients with localized osteosarcoma of the extremity: a joint study by the Italian and Scandinavian Sarcoma Groups. *J Clin Oncol* 2005;23(34):8845–52.
- Flintoff WF, Sadlish H, Gorlick R, Yang R, Williams FM. Functional analysis of altered reduced folate carrier sequence changes identified in osteosarcomas. *Biochim Biophys Acta* 2004;1690(2):110–7.
- Frankel A, Man S, Elliott P, Adams J, Kerbel RS. Lack of multicellular drug resistance observed in human ovarian and prostate carcinoma treated with the proteasome inhibitor PS-341. *Clin Cancer Res* 2000;6(9):3719–28.
- Frankfurt OS, Krishan A. Apoptosis-based drug screening and detection of selective toxicity to cancer cells. *Anticancer Drugs* 2003;14(7):555–61.
- Fujii K, Miyashita T, Takanashi J, Sugita K, Kohno Y, Nishie H, et al. Gamma-irradiation deregulates cell cycle control and apoptosis in nevoid basal cell carcinoma syndrome-derived cells. *Jpn J Cancer Res.* 1999;90(12): 1351–7.
- Hershko A. Roles of ubiquitin-mediated proteolysis in cell cycle control. *Curr Opin Cell Biol* 1997;9(6):788–99.
- Hougardy BMT, Maduro JH, van der Zee AGJ, de Groot DJA, van den Heuvel FAJ, de Vries EGE, et al. Proteasome inhibitor MG132 sensitizes HPV-positive human cervical cancer cells to rhTRAIL-induced apoptosis. *Int J Cancer* 2006;118:1892–900.
- Johnson DE. Noncaspase proteases in apoptosis. *Leukemia* 2000;14(9): 1695–703.
- Kelley TW, Alkan S, Srkalovic G, Hsi ED. Treatment of human chronic lymphocytic leukemia cells with the proteasome inhibitor bortezomib promotes apoptosis. *Leukemia Res* 2004;28(8):845–50.

- Lauricella M, D'Anneo A, Giuliano M, Calvaruso G, Emanuele S, Vento R, et al. Induction of apoptosis in human osteosarcoma Saos-2 cells by the proteasome inhibitor MG132 and the protective effect of pRb. *Cell Death Differ* 2003;10(8):930–2.
- Liu CW, Corboy MJ, DeMartino GN, Thomas PJ. Endoproteolytic activity of the proteasome. *Science* 2003;299(5605):408–11.
- Marina N, Gebhardt M, Teot L, Gorlick R. Biology and therapeutic advances for pediatric osteosarcoma. *Oncologist* 2004;9(4):422–41.
- Merli M, Benassi MS, Gamberi G, Ragazzini P, Sollazzo MR, Molendini L, et al. Expression of G1 phase regulators in MG-63 osteosarcoma cell line. *Int J Oncol* 1999;14(6):1117–21.
- Meyers PA, Gorlick R, Heller G, Casper E, Lane J, Huvos AG, et al. Intensification of preoperative chemotherapy for osteogenic sarcoma: results of the Memorial Sloan-Kettering (T12) protocol. *J Clin Oncol* 1998;16(7):2452–8.
- Miller DK. The role of the caspase family of cysteine proteases in apoptosis. *Semin Immunol* 1997;9:35–49.
- Nahreini P, Andreatta C, Hanson A, Prasad KN. Concomitant differentiation and partial proteasome inhibition trigger apoptosis in neuroblastoma cells. *J Neurooncol* 2003;63(1):15–23.
- Naujokat C, Sezer O, Zinke H, Leclere A, Hauptmann S, Possinger K. Proteasome inhibitors induce caspase-dependent apoptosis and accumulation of p21^{waf1/cip1} in human immature leukemic cells. *Eur J Haematol* 2000;65(4):221–36.
- Rock KL, Gramm C, Rothstein L, Clark K, Stein R, Dick L, et al. Inhibitors of the proteasome block the degradation of most cell proteins and the generation of peptides presented on MHC class I molecules. *Cell* 1994;78(5):761–71.
- Scotlandi K, Serra M, Nicoletti G, Vaccari M, Manara MC, Nini G, et al. Multidrug resistance and malignancy in human osteosarcoma. *Cancer Res* 1996;56(10):2434–9.
- Serra M, Reverter-Branchat G, Maurici D, Benini S, Shen JN, Chano T, et al. Analysis of dihydrofolate reductase and reduced folate carrier gene status in relation to methotrexate resistance in osteosarcoma cells. *Ann Oncol* 2004;15(1):151–60.
- Shah SA, Potter MW, Callery MP. Ubiquitin proteasome pathway: implications and advances in cancer therapy. *Surg Oncol* 2001;10(1–2):43–52.
- Shinoura N, Furitsu T, Asai A, Kirino T, Hamada H. Co-transduction of p27Kip1 strongly augments Fas ligand- and caspase-8-mediated apoptosis in U-373MG glioma cells. *Anticancer Res* 2001;21(5):3261–8.
- Wang J, Lenardo MJ. Roles of caspases in apoptosis, development, and cytokine maturation revealed by homozygous gene deficiencies. *J Cell Sci* 2000;113:753–7.
- Wang X, Gorospe M, Huang Y, Holbrook NJ. P27^{Kip1} overexpression causes apoptotic death of mammalian cells. *Oncogene* 1997;15(24):2991–7.
- Zhou J, Zhang S, Choon-Nam O, Shen HM. Critical role of pro-apoptotic Bcl-2 family members in andrographolide-induced apoptosis in human cancer cells. *Biochem Pharmacol* 2006;72(2):132–44.